HHS Public Access

Author manuscript

Hepatology. Author manuscript; available in PMC 2023 January 01.

Published in final edited form as:

Hepatology. 2022 January ; 75(1): 140–153. doi:10.1002/hep.32148.

Therapeutic Targeting of Hepatic ACSL4 Ameliorates Non-alcoholic Steatohepatitis in Mice

Jingjing Duan[1,*], **Zhuo Wang**[2,*], **Ran Duan**[1,*], **Chenxinhui Yang**[1], **Ruolin Zhao**[1], **Qi Feng**[1], **Yuanyuan Qin**[1], **Jingwei Jiang**[1], **Shouyong Gu**[3], **Kaiyan Lv**[1], **Libo zhang**[1], **Bixia He**[1], **Lutz Birnbaumer**[4], **Song Yang**[5], **Zhen Chen**[1,†], **Yong Yang**[1,†]

[1]Center for New Drug Safety Evaluation and Research, State Key Laboratory of Natural Medicines, China Pharmaceutical University, Nanjing 211198, China.

[2]School of Pharmacy, Nanjing University of Chinese Medicine, Nanjing 210023, China.

[3]Province Geriatic Hospital, 30 Luojia Road, Nanjing 210024, China.

[4]Institute of Biomedical Research (BIOMED), Catholic University of Argentina, Buenos Aires C1107AFF, Argentina, and Neurobiology Laboratory, National Institute of Environmental Health Sciences, Research Triangle Park, North Carolina 27709, USA.

[5]Center of hepatology, Beijing Ditan Hospital of Capital Medical University, Beijing 100015, China.

Abstract

Globally, NAFLD is one of the most common liver disorders, with an estimated prevalence rate of more than 30% in men and 15% in women, and an even higher prevalence in people with type 2 diabetes mellitus. Optimal pharmacologic therapeutic approaches for NAFLD are an urgent necessity. In this study, we showed that compared to healthy controls, hepatic ACSL4 levels in NAFLD patients were found to be elevated. Suppression of ACSL4 expression promoted mitochondrial respiration, thereby enhancing the capacity of hepatocytes to mediate β-oxidation of fatty acids and to minimize lipid accumulation by up-regulating PGC1α. Moreover, we found that abemaciclib is a potent and selective ACSL4 inhibitor, low-dose of abemaciclib significantly ameliorated most of the NAFLD symptoms in multiple NAFLD mice models. Therefore, inhibition of ACSL4 is a potential alternative therapeutic approach for NAFLD.

Keywords

NASH; CDK4/6 inhibitor; PGC1α; Fatty acid β-oxidation; Drug repurposing

[†] Contact Information, Yong Yang, Center for New Drug Safety evaluation and research, State Key Laboratory of Natural Medicines, China Pharmaceutical University, Nanjing 210017, Jiangsu Province P.R.China, yy@cpu.edu.cn, Tel: +86-25-86185622. Zhen Chen, Center for New Drug Safety evaluation and research, State Key Laboratory of Natural Medicines, China Pharmaceutical University, Nanjing 210017, Jiangsu Province P.R.China, czcpu@163.com, Tel: +86-25-025-83271181.

[*]These authors contributed equally to this work.

Introduction

Non-alcoholic fatty liver disease (NAFLD), a hepatic metabolic syndrome, is closely associated with obesity and insulin resistance[1]. Clinically, this syndrome encompasses simple hepatic steatosis, NASH, NASH with fibrosis, and cirrhosis with end-stage liver disease[2, 3]. Globally, NAFLD is gradually becoming a major public health concern that is increasingly being associated with cirrhosis and liver cancer[2].

Currently, lifestyle modification and bariatric surgery are the two most effective and evidence-based therapeutic options for early NASH[4, 5]. However, such non-invasive and straightforward therapies are not overly efficient, especially for NASH with cirrhosis and end-stage liver disease. For NASH regression, it is necessary to lose weight by at least 7% to 10%[6, 7]. However, only 10% of patients can achieve this weight loss objective within one year, and fewer than half of them are able to maintain this weight loss five years later[8]. Studies have aimed at establishing the mechanisms as well as discovering the potential therapeutic targets for NAFLD. Several clinical trials have evaluated novel pharmacological agents that target the multiple pathways involved in NASH's pathogenesis. Saroglitazar, as the first globally authorized non-cirrhotic NASH treatment option, was approved by the Indian Drug Administration in March, 2020. However, its efficacy has not been clearly elucidated. Therefore, new and effective NASH therapies are an urgent necessity.

NAFLD occurs when fatty acid oxidation and lipid exports fail to compensate for increased hepatic uptake of circulating fatty acids and hepatic de novo fatty acid synthesis. Once incorporated into hepatocytes, fatty acids are first converted into acyl-CoA, under the catalysis of acyl-CoA synthetases (ACS), such as acyl-CoA synthetase long-chain family member 4 (ACSL4). ACSL4 has been implicated in several metabolism-associated diseases[9, 10]. ACSL4 knockout cells resist lipid peroxidation by altering their cellular lipid composition[11]. In activated rat hepatic stellate cells, up-regulation was shown to enhance PUFA-TG formation[12]. Moreover, arachidonic acid (AA), an ACSL4 substrate, elevates eicosanoids levels, which promote the secretion of pro-inflammatory cytokines and reactive oxygen species during NAFLD[13]. Human liver fat is significantly correlated with hepatic ACSL4 mRNA expression levels[14, 15]. Under normal physiologic conditions, hepatic ACSL4 levels are low[16], however, under pathological conditions such as NAFLD-HCC, they are significantly up-regulated[17]. Therefore, inhibition of ACSL4 expression or functions in the liver may be a safe strategy for NASH treatment.

In this study, we found that liver-specific ACSL4 deficient mice are resistant to the development of fatty liver and NASH. Importantly, we show that abemaciclib might be a selective inhibitor for ACSL4. Direct pharmacological inhibition of ACSL4 using abemaciclib effectively improved fatty liver and NASH in multiple mice models. Therefore, we validated the hypothesis that ACSL4 may be an alternative target for NASH treatment. This study provides a preclinical basis for repurposing abemaciclib for NASH management.

Materials and Methods

Human liver sections

Human liver sections were obtained from patients who had been subjected to liver biopsy, liver surgery or transplantation. H&E-stained liver sections were independently and blindly scored by two pathologists before immunohistochemical staining of ACSL4. Samples with NASH activity scores (NAS) of 0 were classified as non-steatotic. Samples with a NAS of 1–2, a ballooning score of 0 and no fibrosis were allocated in the simple steatosis group. Samples with NAS > 4 were assigned in the NASH group. All procedures that involved human sample collection were approved by IRB of Beijing Ditan Hospital of Capital Medical University (NO. JDLK-2017–044-01).

Animal studies

C57BL/6 mice and Albumin Cre mice were obtained from Beijing Vital River Laboratory Animal Technology Co. Ltd and from the Shanghai Model Organisms Center, Inc., respectively. Floxed mice were established at the Shanghai Model Organisms Center, Inc., after which they were crossed with Albumin Cre mice through a series of several steps to generate hepatocyte-specific ACSL4 knockout (HepKO) mice. Mice were maintained in environmentally controlled conditions under a 12 h light/dark cycle. Food and water were provided *ad libitum*. Mice were randomly assigned into different experimental groups. Animal experiments were approved by the Institutional Animal Care and Use Committee of the Center for New Drug Safety Evaluation and Research, China Pharmaceutical University.

The HFD-induced fatty liver mice, HepKO mice and Floxed littermate control mice (defined as Flox mice) (male, 6–8 weeks of age) were fed on a HFD diet (60% kcal fat; MD12033, Medicine, Professionals for Lab Animal Diets) for 27 weeks, after which they were sacrificed. Body weights were measured weekly, while blood glucose levels were measured after every two weeks. At the end of experiments, mice were anesthetized and euthanized after blood sampling from the ocular retro-orbital space.

The MCD-induced NASH, HepKO mice and Floxed littermate control mice (defined as Flox mice) (male, 6–8 weeks of age) were fed on an MCD diet (TP3005G, TrophicDiet, Nantong, China) for a period of 8 weeks. At the end of the experiments, mice were anesthetized and euthanized.

The HFF-induced NASH, HepKO mice and Floxed littermate control mice (defined as Flox mice) (male, 7–8 weeks of age) were fed on a HFF diet (42% kcal fat, 42% kcal protein, 42% kcal carbohydrates, 42% kcal cholesterol, TP26304, TrophicDiet, Nantong, China) along with drinking water containing 42 g/L sugar (55% sucrose and 45% fructose by weight) for 16 weeks after which they were sacrificed.

Male 9-week-old C57BL/6 mice were orally administered with 30 mg/kg and 15 mg/kg of abemaciclib or saline control daily, concurrent with the HFF diet. In our pilot study, dose-response evaluations using 15, 30 and 60 mg/kg abemaciclib were performed to investigate its potency. Optimal responses were observed at a dose of 30 mg/kg. Then, we decided to use 15 mg/kg and 30 mg/kg doses in the subsequent experiments. An appropriate volume

of abemaciclib (100 mg/ml stock, in sterile water) was dissolved in a total volume of 240 μL of animal drinking water to achieve a 30 mg/kg body weight/dose, then, diluted further to formulate 15 mg/kg body weight/dose. For the MCD mice models, male 9-week-old C57BL/6 mice were fed on an MCD diet and treated with abemaciclib for 4 weeks as earlier described.

Additional materials and methods are described in the Supplementary Materials and Methods section.

Results

ACSL4 is highly expressed in human NAFLD liver tissues

We used the GSEA gene set enrichment analysis to establish the role of ACSL4 in NAFLD development. Compared to healthy human liver tissues, abnormal fatty acid metabolism was significantly enriched in NAFLD tissues (Fig. 1A). Subsequently, we investigated its expression levels using the Kyoto Encyclopedia of Genes and Genomes (KEGG) and observed that ACSL4 was enriched in fatty acid metabolism pathway-related genes (Fig. 1B). To verify the significance of ACSL4 in NASH, we evaluated its expression levels using three independent Gene Expression Omnibus (GEO) data sets. Expression levels of ACSL4 were significantly up-regulated in NASH (Fig. 1C). Then, we quantified the protein levels of ACSL4 in liver sections of mice after eight weeks of MCD feeding and eighteen weeks of HFF feeding. Fig. 1D shows that, compared to normal mice and to mice fed on the MCS control diet, ACSL4 protein levels were significantly elevated in livers of mice fed on MCD and HFF diet, which was confirmed in human liver tissues as shown in Fig. 1E. To establish which liver cell type mediates the high expression levels of this gene, we analyzed the expression profiles of ACSL4 in mice livers using the Tabula Muris database. Single cell sequencing of mouse tissues revealed that among the top 5 mouse liver cell types, ACSL4 was mainly expressed in hepatocytes (Fig. 1F). These findings support the strong association between liver ACSL4 levels and human NAFLD.

Liver-specific ACSL4 knockout improved HFD diet induced steatosis and MCD diet induced liver fibrosis

Up-regulated expression levels of ACSL4 enhances the development of metabolic syndromes[10]. Based on the significant associations between liver ACSL4 levels and human NAFLD, and the suppressed expression levels of ACSL4 in mice hepatocytes, we evaluated the specific roles of ACSL4 in fatty liver disease using hepatocyte-specific Acsl4-deficient (HepKO) mice. Exon 5 of ACSL4 was deleted via the Cre-LoxP system using a Cre recombinase under the mediation of serum albumin (Alb) gene promoter (Fig. S1A). Then, PCR genotyping of tail tissues were performed (Fig. S1B). Compared to Flox mice, ACSL4 protein levels were found to be significantly suppressed in liver tissues of HepKO mice (Fig. 2A). HepKO mice and its littermate control mice, Flox, had been maintained on a HFD for a period of 27 weeks. In response to prolonged HFD feeding, HepKO mice exhibited a small body weight gain (Fig. 2B), however, blood glucose levels remained unaltered (Fig. 2D), compared to Flox mice. Moreover, compared to the Flox mice, HepKO mice exhibited suppressed hepatic triglyceride levels and reduced liver to body weight ratios (Fig.

2C). Suppressed serum ALT and AST levels further implied protection from lipid-mediated liver damage in HepKO mice (Fig. 2C). Histological analysis of livers showed that hepatic lipid overloading (Fig. 2E) and liver fibrosis (Fig. 2F) were minimal in HepKO mice, when compared to Flox mice. In addition, there were no significant differences in systemic metabolic profiles, including body weights, blood glucose levels, liver to body weight ratios, hepatic triglyceride levels between the two groups when they were fed on a normal diet (Fig. S2A–F).

Liver-specific ACSL4 knockout improved HFF-diet induced liver fibrosis

Since NASH is an advanced form of NAFLD, with an increased probability of progressing to high-burden conditions such as cirrhosis, end-stage liver disease, and hepatocellular carcinoma (HCC)[18], we determined whether a loss of ACSL4 impacts liver fibrosis. HepKO and Flox mice were maintained on a fructose-rich HFF diet for 16 weeks. Consistent with previous findings, after 16 weeks of HFF feeding, HepKO mice exhibited a low body weight gain (Fig. 3A), low hepatic triglyceride levels, as well as reduced liver to body weight ratios (Fig. 3B). These effects were not observed in Flox mice. Liver fibrosis was evaluated by Sirius red staining. As with liver steatosis, compared to control mice, HepKO mice exhibited less fibrosis and showed an attenuated hepatic lipid accumulation (Fig. 3E). Histopathologic improvement was correlated with low ALT and AST levels (Fig. 3C). There were no significant deviations in blood glucose levels (Fig. 3D). These findings show that in response to HFF diet treatment, ACSL4 played a critical role in regulating mice liver fibrosis. Therefore, hepatocyte-specific loss of ACSL4 may protect mice from developing NASH.

Pharmacologic inhibition of ACSL4 expression improved steatosis and liver fibrosis

The above findings show that ACSL4 is a potential therapeutic target for NAFLD. Therefore, we determined whether pharmacologic inhibition of ACSL4 is a potential therapeutic target for NASH treatment. To establish the pharmacologic inhibitors of ACSL4, we performed molecular docking by executing machine-learning and deep-learning approaches to predict the binding affinity between ACSL4 and various compounds. Eighteen potential compounds interacted with the binding site of ACSL4 (Fig. S3A). Among them, compared to other known ACSL4 inhibitors[11] such as troglitazone (−10 kcal/mol), rosiglitazone (−8.4 kcal/mol) and pioglitazone (−9.1 kcal/mol), abemaciclib exhibited the highest docking score (−12.8 kcal/mol) (Fig. S3A). To verify that ACSL4 is a direct target for abemaciclib, we performed the microscale thermophoresis (MST) assay, which confirmed the binding of abemaciclib and troglitazone, with dissociation constants (Kd) of 146.34 μM and 180.44 μM respectively (Fig. 4A). To determine whether these compounds regulate ACSL4 expression, we evaluated the expressions of twelve compounds using Western blot (Fig. S3B). Three compounds were found to suppress ACSL4 protein levels, among which abemaciclib was the most significant (Fig. S3B). These findings imply that abemaciclib is a potent and selective inhibitor for ACSL4.

Given that NASH is a more serious stage of NAFLD, we determined whether abemaciclib treatment is effective in HFF induced NASH mice models. For a period of ten weeks, abemaciclib (15 mg/kg or 30 mg/kg per day) was orally administered along with the

HFF diet. Mice fed on HFF and administered with equivalent amounts of animal drinking water were used as controls. In HepKO mice, there was a significant reduction in hepatic lipid accumulation as evidenced by Oil red O staining (Fig. 4B). Significantly attenuated hepatic fibrosis in abemaciclib treated mice was shown by Sirius red staining and immunohistochemical staining of α-SMA (Fig. 4C). Despite the reduction in body weights gain and ACSL4 protein levels in 30 mg/kg abemaciclib administered mice (Fig. 4D), there were no significant differences in blood glucose levels among groups (data not shown). In accordance with low hepatic steatosis and liver fibrosis findings, livers from abemaciclib treated mice exhibited less hepatocyte injuries as indicated by low serum AST levels (Fig. 4F). Serum ALT levels were slightly decreased in abemaciclib treated group, however, there were no statistical differences among groups (Fig. 4F). Compared to control mice, mice treated with abemaciclib (30 mg/g per day) exhibited significantly suppressed hepatic triglyceride levels as well as reduced liver to body weight ratios (Fig. 4E). Therefore, suppressing ACSL4 expression in the liver by administering abemaciclib is an effective way for inhibiting liver steatosis and NASH development.

ACSL4 knockdown enhanced mitochondrial respiration by promoting fatty acid oxidation without promoting oxidative stress induced cytotoxicity

Although initial causes of NAFLD have not been elucidated, pathological accumulation of lipids in the liver has been shown to be a consequence of lipid accumulation exceeding lipid disposal levels[19]. Mitochondrial fatty acid β-oxidation is a major pathway for fatty acid catabolism. To establish the mechanisms through which ACSL4 silencing suppresses lipid accumulation, we first performed the Seahorse Mito Stress assay to determine whether ACSL4 silencing enhances mitochondrial respiration in HepG2 cells. The oxygen consumption rate (OCR) was found to be elevated in ACSL4 silenced cells with increased basal respiration, maximal respiration, and ATP-production-coupled respiration compared to control cells (Fig. 5A). Comparable findings were observed in human primary hepatocyte-derived liver progenitor-like cells (HepLPCs) (Fig. 5C). Mitochondrial membrane potential was also elevated in ACSL4 silenced HepG2 cells and HepLPCs cells (Fig. 5B and D). Consistent with these findings, expression levels of genes involved in mitochondrial fatty acid oxidation (PPARα, PGC1α, CPT1A, ACC2, and ACADL) were found to be elevated, but lipogenesis associated genes (ACC1, FASN, and SREBP1) were suppressed in ACSL4 silenced cells (Fig. 5E). PGC1α levels in ACSL4 silenced cells or in abemaciclib treated HepG2 cells were confirmed by Western blot. Consistent with mRNA expression levels, ACSL4 protein levels were elevated in both ACSL4 silenced and abemaciclib treated HepG2 cells (Fig. 5F). Subsequent *in vivo* experiments validated these *in vitro* findings. It was shown that PGC1α protein levels were elevated in ACSL4 deficient mice fed on normal and HFF diets (Fig. 5F) as well as in abemaciclib treated mice fed on a HFF diet (Fig. 5F). Therefore, suppression of ACSL4 enhances mitochondrial respiration and promotes fatty acid oxidation.

Enhanced β-oxidation elevates reactive oxygen species (ROS) production[20], leading to lipid peroxidation and cell death. To exclude this possibility, we evaluated lipid ROS levels using BODIPY 581/591 C11, a lipid peroxidation sensor used to detect ROS in cells and membranes. Despite elevated fatty acid oxidation and mitochondrial respiration, ROS levels

in ACSL4 silenced HepG2 cells were lower than those of control cells (Fig. 6A). To confirm cellular antioxidant defenses in ACSL4 silenced HepG2 cells (Fig. 6C and D) and in mouse primary hepatocytes derived from the livers of HepKO and Flox mice (Fig. 6B), a panel of fatty acids, including docosahexaenoic acid (DHA), arachidonic acid (AA), and hydrogen peroxide (H_2O_2) were supplemented in the cell culture medium at increasing concentrations for 48 h, after which cell viabilities were assessed via the CCK-8 staining assay (Cell counting kit-8). Fig. 6B–E shows that ACSL4 knock down cells were significantly protected from H_2O_2, DHA, and AA-induced cell death in a dose-dependent manner, which may not be related with apoptosis (Fig. S5). These results suggest that targeting ACSL4 in the liver is an alternative approach for treating NASH, as it prevents lipid accumulation by boosting mitochondrial respiration and β-oxidation without elevating ROS production.

Hexadecanamide was enriched among hepatic metabolites in HepKO mice and could activate PPARα

Our findings imply that ACSL4 knock-down in HepG2 cells can significantly elevate PPARα expression. The peroxisome proliferator-activated receptor α (PPARα), is a ligand-activated transcription factor that is involved in various biological processes, including fatty acid metabolism[21]. Endogenous ligands have a low adverse potential, and therefore, offer much better therapeutic strategies[22]. Therefore, we investigated the existence of endogenous ligands of PPARα in the liver. Then, we performed widely targeted metabolomics analysis of metabolites from liver samples of HepKO and Flox mice, after which we generated a list with fold-changes and *p*-values for each metabolite (Fig. S6A and B). Among all the significantly up-regulated metabolites (Fig. 7A and B), hexadecanamide has previously been shown to serve as an endogenous PPARα ligand in mouse brain hippocampus[22, 23]. Therefore, it was of interest to establish whether hexadecanamide regulates the activity of PPARα in the liver and, thereby, altering the expression levels of PPARα target genes. HepG2 cells were challenged with hexadecanamide at doses of 2.5 μM and 10 μM. After 48 h, we measured mRNA expression levels of PPARα and PPARα target genes, including FGF21, FSP27, and VNN1, since these genes are strictly PPARα dependent[24]. We found that, compared to controls, hexadecanamide enhanced their expression levels in a dose-dependent manner (Fig. 7C). We further evaluated the protein levels of PPARα after hexadecanamide challenge *in vitro*. Expression levels of the PPARα protein and those of its co-activator, PGC1α, a transcriptional co-activator that regulates several key hepatic metabolic pathways, especially fatty acid oxidation were found to be elevated (Fig. 7D). These results imply that hexadecanamide enhances hepatocyte PPARα activities. It has been reported that the PGC1α-PPARα axis increases the hepatic capacity for mitochondrial fatty acid oxidation[25], while hepatocyte PPARα is required for protection against steatohepatitis[24–26]. Compared to control cells, cells treated with 10 μM hexadecanamide significantly attenuated free fatty acid induced lipid accumulation (Fig. 7E). However, there were no significant differences in lipid accumulation levels in cells treated with DL-Benzylsuccinic acid, m-Coumaric acid and γ-Glutamate-Cysteine (Fig. S6C). These results show that ACSL4 inhibition may be beneficial in NASH by inducing the production of the hepatic metabolite, hexadecanamide, which functions to enhance hepatocyte PPARα activities together with PGC1a.

ACSL4 regulates fatty acid oxidation through the TGF-β1/ Smad3/PGC1α axis.

It has been reported that Smad3 suppresses PGC-1α expression, the loss of which protects against diet-induced obesity and hepatic steatosis[27]. We found that phosphorylation of Smad3 was significantly inhibited by silencing ACSL4 (Fig. 8A). Comparable to findings from ACSL4 knock down cells, HepG2 cells treated with abemaciclib exhibited suppressed expression levels of phosphorylated Smad3 (Fig. 8B), indicating that ACSL4 knockdown promotes PGC1α expression in a Smad3-dependent manner. Since Smad3 serves as a principal facilitator of TGF-β signals, it is necessary to explore that TGF-β may be involved in the regulation of ACSL4. As shown in Fig. 8C, protein levels of ACSL4 were elevated in the presence of TGF-β1, but were significantly suppressed when Smad3 was pharmacologically inhibited with the Smad3 inhibitor (SIS3; Fig. 8D). These results indicate that ACSL4 may regulate fatty acid oxidation through the TGF-β1/ Smad3/PGC1α axis.

Discussion

Globally, NAFLD is a public health problem that is increasingly becoming common, and is among the leading causes of chronic liver disease. It is estimated that in the next decade, NASH incidences will increase by 56%[28]. Due to advances in molecular and genetic profiling, numerous pathogenic molecular pathways involved in NASH development and progression have been identified. Currently, lifestyle interventions are the primary therapeutic options for NASH. Moreover, several pharmacologic options such as insulin sensitizers(metformin, troglitazone)[29, 30] lipid-lowering agents (gemfibrozil)[31], and antioxidants (vitamin E)[32] are used for NASH management, and their applications are limited by weak efficacies or long-term side effects.

Thiazolidinediones, such as rosiglitazone, pioglitazone, and troglitazone, specifically inhibit ACSL4 over other ACSL isoforms[33]. In this study, molecular docking revealed that abemaciclib has a more potent binding affinity than the other ACSL4 inhibitors. Pioglitazone has been shown to be efficacious in treating NASH, and exerts beneficial effects on lipids. However, its clinical applications may be limited by various side effects, including fluid retention and weight gain[34]. We found that pharmacologic inhibition of the expression of ACSL4 by administering abemaciclib at 30 mg/kg per day significantly suppressed body weights and improved NASH-assocoated pathological features, including hepatic steatosis and fibrosis. In 2017, Abemaciclib was approved by the United States Food and Drug Administration (FDA) to treat hormone receptor-positive and HER2-negative breast cancer. Compared to the other two CDK4/6 inhibitors, abemaciclib is the only CDK4/6 inhibitor that can be used as a single therapy with milder neutropenia, no need for any drug holiday or long-term medication[35, 36].

Abemaciclib inhibits tumor cell proliferation by activating CDK4/6, and thereby, phosphorylating the retinoblastoma (RB1) family of proteins[37]. Despite the requirement of kinase activity, involvement of CDK4/6 can be separated from its classical role in cell cycle regulation and RB1 phosphorylation[38–40.] As a potent, selective CDK4/6 kinase inhibitor, abemaciclib suppressed RB1 phosphorylation in HepG2 cells. As did the other CDK4/6 approved inhibitors, including palbociclib and ribociclib (Fig. S3C). Although they inhibited RB1 phosphorylation in a dose-dependent manner, suppressed ACSL4 protein levels were

observed, particularly in response to abemaciclib (Fig. S3C). Corresponding results were observed at mRNA expression levels of ACSL4, which were suppressed upon treatment with abemaciclib (Fig. S3D). Molecular docking did not show a docking score for the other two above mentioned CDK4/6 inhibitors (data not shown). Moreover, CDK4/6 knockdown using shRNA did not affect cellular lipid deposition in HepG2 cells treated with abemaciclib (Fig. S4). Collectively, these findings imply that abemaciclib has unique pharmacological properties that are not shared with the other potent CDK4/6 kinase inhibitors, palbociclib and ribociclib. Therapeutic effects of abemaciclib on NASH involve ACSL4, and may be independent of the CDK4/6-RB1 pathway.

Excess lipids accumulation in hepatocytes and lipid peroxidation are typical NAFLD characteristics. NASH progression is enhanced by ROS-induced lipotoxicity. Elevated fatty acid metabolism can suppress cytoplasmic lipid accumulation in the liver, and therefore, reduce lipotoxicity. Accordingly, promotion of mitochondrial function and enhancement of fatty acid oxidation is the most efficient strategy for reducing lipotoxicity. However, elevated β-oxidation levels are associated with increased ROS production with the potential for oxidative damage. In this study, ACSL4 deficiency was shown to protect cells from H_2O_2 and polyunsaturated fatty acid-induced cell death, without inducing cellular ROS accumulation. Sebastian Doll et al. reported similar results that ACSL4 deficient tumor cells are refractory to lipid peroxidation, which protects cells from death[11]. In this study, therapeutic inhibition of ACSL4 improved hepatic lipid accumulation, probably by enhancing mitochondrial function and, thereby, boosting lipid catabolism. Even though the effects of ACSL4 inhibition on NAFLD can help inform potential therapeutic strategies, we did not establish why enhanced mitochondrial β-oxidation when ACSL4 was inhibited did not increase cellular ROS production, but protected cells from peroxide-induced death. One explanation could be that, since ACSL4 is involved in the synthesis of membrane phospholipids, which are rich in long-chain polyunsaturated fatty acids, they can be oxidized to initiate membrane lipid ROS accumulation[11]. Studies have also shown that elevated Complex I activity promotes mitochondrial respiration, without elevating mitochondrial ROS production[41].

In this study, we show that abemaciclib exerted a therapeutic effect against NASH through the ACSL4/PGC1α axis, which maybe a novel kinase-independent action. Our findings show the therapeutic potential of ACSL4 for the treatment of NASH and provides evidence that abemaciclib is a potent and selective ACSL4 inhibitor. These findings provide a preclinical basis for repurposing of abemaciclib into clinical trials for NASH management.

Supplementary Material

Refer to Web version on PubMed Central for supplementary material.

Acknowledgments

Financial Support

This study was supported by the National Natural Science Foundation of China (Nos. 81673468, 82003788, 82073280), the National Key New Drug Innovation Program, the Ministry of Science and Technology of China (No: 2018ZX09201017–006), “Double First-Class” University Project (No. CPU2018GF10 and CPU2018GY46),

the Scientific Startup Foundation for High level Scientists of China Pharmaceutical University (No. 3154070026), the Natural Science Foundation of Jiangsu province (BK20190801), Youth Project of Natural Science Foundation of Nanjing University of Chinese Medicine (NZY82003788), The Intramural Research Program of the NIH (Project Z01-ES-101684 to LB), and the National Institutes of Health (NIH) Intramural Research Program (Project ES-101643 to LB).

List of Abbreviations

NAFLD	Non-alcoholic fatty liver disease
NASH	Nonalcoholic steatohepatitis
AA	Arachidonic acid
PUFA-TG	Polyunsaturated fatty acid-Triglycerides
PGC1α	Peroxisome proliferator activated receptor coactivator-1 alpha
GSEA	Gene set enrichment analysis
KEGG	Kyoto Encyclopedia of Genes and Genomes
GEO	Gene Expression Omnibus
MCD	Methionine-choline deficient diet
HFF	High fat-high cholesterol and high fructose diet
HepKO	Hepatocyte-specific Acsl4-deficient mice
Floxed	Hepatocyte-specific Acsl4-Floxed mice
ALT	Alanine aminotransferase
AST	Aspartate aminotransferase
HCC	Hepatocellular carcinoma
HFD	Hight fat diet
DHA	Docosahexaenoic acid

References

1. Ayako Suzuki AMD. Nonalcoholic Steatohepatitis. Annu Rev Med 2017 68:85–98. [PubMed: 27732787]
2. Laurent Castera MF-R, Rohit Loomba Noninvasive Assessment of Liver Disease in Patients With Nonalcoholic Fatty Liver Disease. Gastroenterology 2019;156:1264–1281. [PubMed: 30660725]
3. Timothy Hardy FO, Anstee Quentin M, Day Christopher P Nonalcoholic Fatty Liver Disease: Pathogenesis and Disease Spectrum. Annu Rev Pathol 2016;11:451–496. [PubMed: 26980160]
4. Guillaume Lassailly RC, Ntandja-Wandji Line-Carolle, Gnemmi Viviane, Baud Gregory, Verkindt Helene, Ningarhari Massih, Louvet Alexandre, Leteurtre Emmanuelle, Violeta Raverdy, Dharancy Sébastien, Pattou François, Mathurin Philippe Bariatric Surgery Provides Long-term Resolution of Nonalcoholic Steatohepatitis and Regression of Fibrosis. Gastroenterology 2020;159:1290–1301.e1295. [PubMed: 32553765]

5. Zobair M Younossi KEC, Lim Joseph K AGA Clinical Practice Update on Lifestyle Modification Using Diet and Exercise to Achieve Weight Loss in the Management of Nonalcoholic Fatty Liver Disease (NAFLD): Expert Review. Gastroenterology 2020:S0016–5085(0020)35538–35534.
6. Eduardo Vilar-Gomez YM-P, Calzadilla-Bertot Luis, Torres-Gonzalez Ana, Gra-Oramas Bienvenido, Gonzalez-Fabian Licet, Friedman Scott L, Diago Moises, Romero-Gomez Manuel Weight Loss Through Lifestyle Modification Significantly Reduces Features of Nonalcoholic Steatohepatitis. Gastroenterology 2015;149:367–378.e365. [PubMed: 25865049]
7. Kittichai Promrat DEK, Niemeier Heather M, Jackvony Elizabeth, Kearns Marie, Wands Jack R, Fava Joseph L, Wing Rena R. Randomized controlled trial testing the effects of weight loss on nonalcoholic steatohepatitis. Hepatology 2010;51:121–129. [PubMed: 19827166]
8. Rena R Wing SP. Long-term weight loss maintenance. Am J Clin Nutr 2005;82:222S–225S. [PubMed: 16002825]
9. Yang Li DF, Wang Zhanyu, Zhao Yan, Sun Ruimin, Tian Donghai, Liu Deshun, Zhang Feng, Ning Shili, Yao Jihong, Tian Xiaofeng Ischemia-induced ACSL4 activation contributes to ferroptosis-mediated tissue injury in intestinal ischemia/reperfusion. Cell Death Differ 2019;26:2284–2299. [PubMed: 30737476]
10. Elizabeth A Killion ARR, El Azzouny Mahmoud A, Yan Qing-Wu, Surujon Defne, Griffin John D, Bowman Thomas A, Wang Chunyan, Matthan Nirupa R, Klett Eric L, Kong Dong, Newman John W, Han Xianlin, Lee Mi-Jeong, Coleman Rosalind A, Greenberg Andrew S A role for long-chain acyl-CoA synthetase-4 (ACSL4) in diet-induced phospholipid remodeling and obesity-associated adipocyte dysfunction. Mol Metab 2018;9.
11. Sebastian Doll BP, Tyurina Yulia Y, Panzilius Elena, Kobayashi Sho, Ingold Irina, Irmler Martin, Beckers Johannes, Aichler Michaela, Walch Axel, Prokisch Holger, Trümbach Dietrich, Mao Gaowei, Qu Feng, Bayir Hulya, Füllekrug Joachim, Scheel Christina H, Wurst Wolfgang, Schick Joel A, Kagan Valerian E, Angeli José Pedro Friedmann, Conrad Marcus. ACSL4 dictates ferroptosis sensitivity by shaping cellular lipid composition. Nat Chem Biol 2017;13:91–98. [PubMed: 27842070]
12. Maidina Tuohetahuntila BS, Kruitwagen Hedwig S, Wubbolts Richard, Brouwers Jos F, van de Lest Chris H, Molenaar Martijn R, Houweling Martin, Helms J Bernd, Vaandrager Arie B Role of long-chain acyl-CoA synthetase 4 in formation of polyunsaturated lipid species in hepatic stellate cells. Biochim Biophys Acta 2015;1851:220–230. [PubMed: 25500141]
13. Progga Sen CFKK, Singh Amar B, Rius Monica, Kraemer Fredric B, Sztul Elizabeth, Liu Jingwen Identification of p115 as a novel ACSL4 interacting protein and its role in regulating ACSL4 degradation. J Proteomics 2020;229:103926. [PubMed: 32736139]
14. Anna Kotronen HY-J, Aminoff Anna, Bergholm Robert, Pietiläinen Kirsi H, Westerbacka Jukka, Talmud Philippa J, Humphries Steve E, Hamsten Anders, Isomaa Bo, Groop Leif, Orho-Melander Marju, Ehrenborg Ewa, Fisher Rachel M. Genetic variation in the ADIPOR2 gene is associated with liver fat content and its surrogate markers in three independent cohorts. Eur J Endocrinol 2009;160:593–602. [PubMed: 19208777]
15. Jukka Westerbacka MK, Kiviluoto Tuula, Arkkila Perttu, Sirén Jukka, Hamsten Anders, Fisher Rachel M, Yki-Järvinen Hannele. Genes involved in fatty acid partitioning and binding, lipolysis, monocyte/macrophage recruitment, and inflammation are overexpressed in the human fatty liver of insulin-resistant subjects. Diabetes 2007;56:2759–2765. [PubMed: 17704301]
16. Y Cao ET, Zimmerman GA, McIntyre TM, Prescott SM. Cloning, Expression, and Chromosomal Localization of Human Long-Chain Fatty Acid-CoA Ligase 4 (FACL4). Genomics 1998;49:327–330. [PubMed: 9598324]
17. Dabin Liu CCW, Fu Li, Chen Huarong, Zhao Liuyang, Li Chuangen, Zhou Yunfei, Zhang Yanquan, Xu Weiqi, Yang Yidong, Wu Bin, Cheng Gong, Lai Paul Bo-San, Wong Nathalie, Sung Joseph J Y, Yu Jun Squalene epoxidase drives NAFLD-induced hepatocellular carcinoma and is a pharmaceutical target. Sci Transl Med 2018;10:eaap9840. [PubMed: 29669855]
18. Catherine Frenette ZK, Mena Edward, Mantry Parvez S, Lucas Kathryn J, Neff Guy, Rodriguez Miguel, Thuluvath Paul J, Weinberg Ethan, Bhandari Bal R, Robinson James, Wedick Nicole, Chan Jean L, Hagerty David T, Kowdley Kris V, IDN-6556–17 Study Investigators. Emricasan to prevent new decompensation in patients with NASH-related decompensated cirrhosis. J Hepatol 2020;S0168–8278:33673–33674.

19. Jin Young Huh SMR, Abu-Odeh Mohammad, Murphy Anne N, Mahata Sushil K, Zhang Jinyu, Cho Yoori, Seo Jong Bae, Hung Chao-Wei, Green Courtney R, Metallo Christian M, Saltiel Alan R. TANK-Binding Kinase 1 Regulates the Localization of Acyl-CoA Synthetase ACSL1 to Control Hepatic Fatty Acid Oxidation. Cell Metab 2020 12 1;32(6):1012–1027e7 2020;32:1012–1027.e1017. [PubMed: 33152322]
20. Anabela P Rolo JST, Palmeira Carlos M. Role of oxidative stress in the pathogenesis of nonalcoholic steatohepatitis. Free Radic Biol Med 2012;52:59–69. [PubMed: 22064361]
21. Michal Pawlak PL, Staels Bart. Molecular mechanism of PPARα action and its impact on lipid metabolism, inflammation and fibrosis in non-alcoholic fatty liver disease. J Hepatol 2015;62:720–733. [PubMed: 25450203]
22. Dhruv Patel AR, Raha Sumita, Kundu Madhuchhanda, Gonzalez Frank J, Pahan Kalipada. Upregulation of BDNF and hippocampal functions by a hippocampal ligand of PPARα. JCI Insight 2020;5:e136654.
23. Avik Roy MK, Jana Malabendu, Mishra Rama K, Yung Yeni, Luan Chi-Hao, Gonzalez Frank J, Pahan Kalipada. Identification and characterization of PPARα ligands in the hippocampus. Nat Chem Biol 2016;12:1075–1083. [PubMed: 27748752]
24. Alexandra Montagner AP, Fouché Edwin, Ducheix Simon, Lippi Yannick, Lasserre Frédéric, Barquissau Valentin, Régnier Marion, Lukowicz Céline, Benhamed Fadila, Iroz Alison, Bertrand-Michel Justine, Al Saati Talal, Cano Patricia, Mselli-Lakhal Laila, Mithieux Gilles, Rajas Fabienne, Lagarrigue Sandrine, Pineau Thierry, Loiseau Nicolas, Postic Catherine, Langin Dominique, Wahli Walter, Guillou Hervé. Liver PPARα is crucial for whole-body fatty acid homeostasis and is protective against NAFLD. Gut 2016;65:1202–1214. [PubMed: 26838599]
25. Brian N Finck MCG, Chen Zhouji, Leone Teresa C, Croce Michelle A, Harris Thurl E, Lawrence John C Jr, Kelly Daniel P. Lipin 1 is an inducible amplifier of the hepatic PGC-1alpha/PPARalpha regulatory pathway. Cell Metab 2006;4:199–210. [PubMed: 16950137]
26. Elena Piccinin GV, Moschetta Antonio. Metabolic aspects in NAFLD, NASH and hepatocellular carcinoma: the role of PGC1 coactivators. Nat Rev Gastroenterol Hepatol 2019;16:160–174. [PubMed: 30518830]
27. Hariom Yadav CQ, Kamaraju Anil K, Gavrilova Oksana, Malek Rana, Chen Weiping, Zerfas Patricia, Zhigang Duan, Wright Elizabeth C, Stuelten Christina, Sun Peter, Lonning Scott, Skarulis Monica, Sumner Anne E, Finkel Toren, Rane Sushil G. Protection from obesity and diabetes by blockade of TGF-β/Smad3 signaling. Cell Metab 2011;14:67–79. [PubMed: 21723505]
28. Daniel Q Huang HBE-S, Loomba Rohit. Global epidemiology of NAFLD-related HCC: trends, predictions, risk factors and prevention. Nat Rev Gastroenterol Hepatol 2020.
29. G Marchesini MB, Bianchi G, Tomassetti S, Zoli M, Melchionda N. Metformin in non-alcoholic steatohepatitis. Lancet 2001;358:893–894. [PubMed: 11567710]
30. S H Caldwell EEH, Redick JA, Iezzoni JC, Battle EH, Sheppard BL. A pilot study of a thiazolidinedione, troglitazone, in nonalcoholic steatohepatitis. Am J Gastroenterol 2001;96:519–525. [PubMed: 11232700]
31. M Basaranoglu OA, Sonsuz A. A controlled trial of gemfibrozil in the treatment of patients with nonalcoholic steatohepatitis. J Hepatol 1999;31:384. [PubMed: 10453959]
32. T Hasegawa MY K Nakamura, Makino, A Terano. Plasma transforming growth factor-beta1 level and efficacy of alpha-tocopherol in patients with non-alcoholic steatohepatitis: a pilot study. Aliment Pharmacol Ther 2001;15:1667–1672. [PubMed: 11564008]
33. J H Kim TML, Coleman RA. Expression and characterization of recombinant rat Acyl-CoA synthetases 1, 4, and 5. Selective inhibition by triacsin C and thiazolidinediones. J Biol Chem 2001;276:24667–24673. [PubMed: 11319222]
34. Margery A Connelly JVR, Guyton John R, Siddiqui Mohammad Shadab, Sanyal Arun J. Review article: the impact of liver-directed therapies on the atherogenic risk profile in non-alcoholic steatohepatitis. Aliment Pharmacol Ther 2020;52:619–636. [PubMed: 32638417]
35. Kim ES. Abemaciclib: First Global Approval. Drugs 2017;77:2063–2070. [PubMed: 29128965]
36. Charles J Sherr DB, Shapiro Geoffrey I Targeting CDK4 and CDK6: From Discovery to Therapy. Cancer Discov 2016;6:353–367. [PubMed: 26658964]

37. Erika Hamilton JRI. Targeting CDK4/6 in patients with cancer. Cancer Treat Rev 2016;45:129–138. [PubMed: 27017286]

38. Michele Dowless CDL, Shackleford Terry, Renschler Matthew, Stephens Jennifer, Flack Robert, Blosser Wayne, Gupta Simone, Stewart Julie, Webster Yue, Dempsey Jack, VanWye Alle B, Ebert Philip, Iversen Philip, Olsen Jonathan B, Gong Xueqian, Buchanan Sean, Houghton Peter, Stancato Louis. Abemaciclib Is Active in Preclinical Models of Ewing Sarcoma via Multipronged Regulation of Cell Cycle, DNA Methylation, and Interferon Pathway Signaling. Clin Cancer Res 2018;24:6028–6039. [PubMed: 30131386]

39. Marc Hafner CEM, Subramanian Kartik, Chen Chen, Chung Mirra, Boswell Sarah A, Everley Robert A, Liu Changchang, Walmsley Charlotte S, Juric Dejan, Sorger Peter K Multiomics Profiling Establishes the Polypharmacology of FDA-Approved CDK4/6 Inhibitors and the Potential for Differential Clinical Activity. Cell Chem Biol 2019;26:1067–1080.e1068. [PubMed: 31178407]

40. Mary E. Klein MK, Davis Lara E., Tap William D., and Koff Andrew,. CDK4/6 inhibitors: The mechanism of action may not be as simple as once thought. Cancer Cell 2018;34:9–20. [PubMed: 29731395]

41. Lucía Barbier-Torres KAF, Iruzubieta Paula, Delgado Teresa C, Giddings Emily, Chen Youdinghuan, Champagne Devin, Fernández-Ramos David, Mestre Daniela, Gomez-Santos Beatriz, Varela-Rey Marta, de Juan Virginia Gutiérrez, Fernández-Tussy Pablo, Zubiete-Franco Imanol, García-Monzón Carmelo, González-Rodríguez Águeda, Oza Dhaval, Valença-Pereira Felipe, Fang Qian, Crespo Javier, Aspichueta Patricia, Tremblay Frederic, Christensen Brock C, Anguita Juan, Martínez-Chantar María Luz, Rincón Mercedes. Silencing hepatic MCJ attenuates non-alcoholic fatty liver disease (NAFLD) by increasing mitochondrial fatty acid oxidation. Nat Commun 2020;11:3360. [PubMed: 32620763]

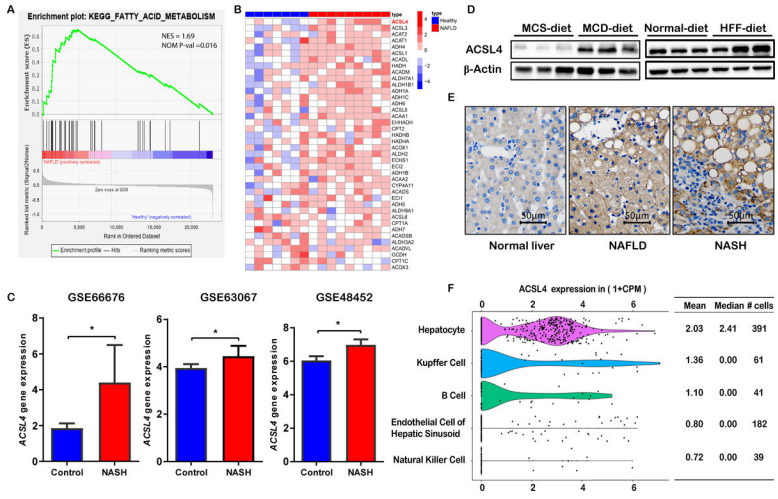

Fig. 1. Elevated ACSL4 expression levels in the liver are correlated with NAFLD development in humans.

(A) GSEA pathway enrichment results showing the cellular pathways enriched in lipid metabolism. Transcriptomic data of NAFLD patients and control adults was obtained from the publically available GEO database (GSE63067). Control, n=7; NAFLD, n=11. (B) Heatmap showing the expression profiles of lipid metabolism associated genes that were up-regulated in NAFLD. Control, n=7; NAFLD, n=11. (C) Effects of ACSL4 on NASH development as revealed using three independent Gene Expression Omnibus (GEO) data sets. GSE66676 (Control, n=34; NASH, n=7), n= GSE63067 (Control, n=7; NASH, n=11), GSE48452 (Control, n=14; NASH, n=18). (D) ACSL4 expressions in non-steatosis or NASH mice liver. (E) ACSL4 expressions in human livers with non-steatotic (n=2), simple steatosis (n=3) and NASH (n=3). (F) Expression profileS of ACSL4 in mice liver. Scale bars indicate 50 μm. Error bars represent mean±SD. *denotes $p < 0.05$.

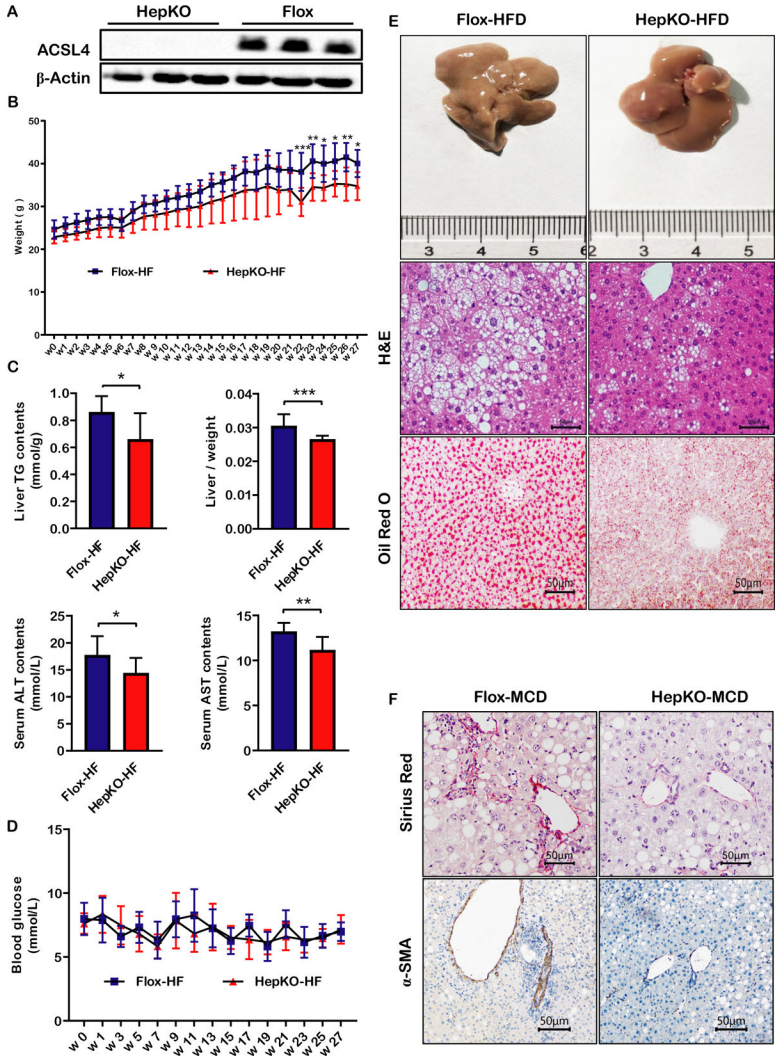

Fig. 2. ACSL4 deficient mice fed on a HFD and MCD are resistant to liver steatosis and fibrosis development.

(A) ACSL4 protein levels in livers of Flox and HepKO mice fed on a normal diet were evaluated by Western blot. n=3 per group. (B) Body weight changes in Flox and HepKO mice fed on a HFD (60% high fat diet) diet at indicated time points. n=10 per group. (C) Hepatic triglyceride levels, liver to weight ratios as well as serum ALT and AST levels in Flox and HepKO mice fed on a HFD diet for 27 weeks. Mice livers and serum were obtained after overnight fasting. n=10 per group. (D) Blood glucose changes in Flox and HepKO mice fed on a HFD diet for 27 weeks. n=10 per group. (E) Representative macroscopic images, liver H&E images and liver lipid contents for Flox and HepKO mice fed on a HFD for 27 weeks as determined by Oil red O staining. n=6 per group. (F) Representative liver fibrosis for mice fed on methionine-choline deficient diet (MCD) for 8 weeks as determined by Sirius Red staining and α-SMA staining. Scale bars indicate 50 μm. n=6 per group. Error bars represent mean±SD. *denotes $p < 0.05$, **denotes $p < 0.01$, ***denotes $p < 0.005$.

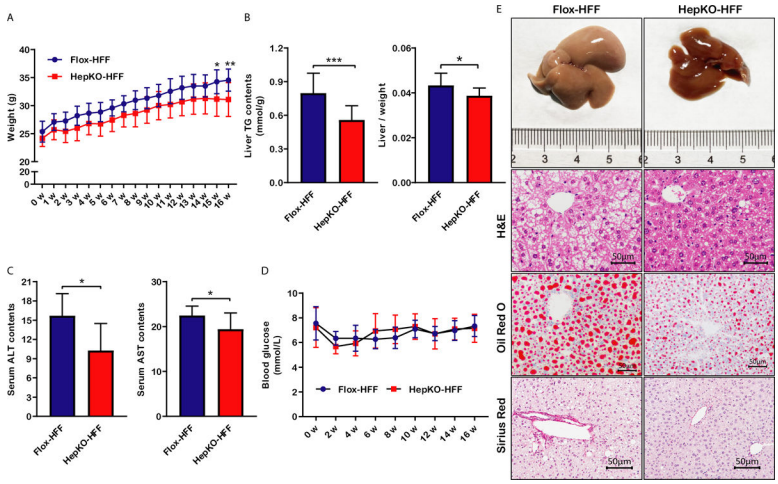

Fig. 3. ACSL4 deficient mice fed on a HFF diet are resistant to liver steatosis and fibrosis development.

Flox and HepKO mice were fed on a high fat-high cholesterol and high fructose (HFF) diet for 16 weeks. Their livers and serum were obtainted after overnight fasting. (A) Body weight changes at indicated time points. n=10 per group. (B) Hepatic triglyceride levels, liver to weight ratios in Flox and HepKO mice fed on a HFF diet. n=10 per group. (C) Serum ALT and AST levels in Flox and HepKO mice fed on a HFF diet. n=8 per group. (D) Blood glucose levels in Flox and HepKO mice fed on a HFF diet. n=10 per group. (E) Representative macroscopic images, liver H&E images, and liver lipid levels in Flox and HepKO mice fed on a HFF diet as determined by Oil red O staining and liver fibrosis as determined by Sirius Red staining. n=10 per group. Scale bars indicate 50 μm.. Error bars represent mean±SD. *denotes $p < 0.05$, ***denotes $p < 0.005$.

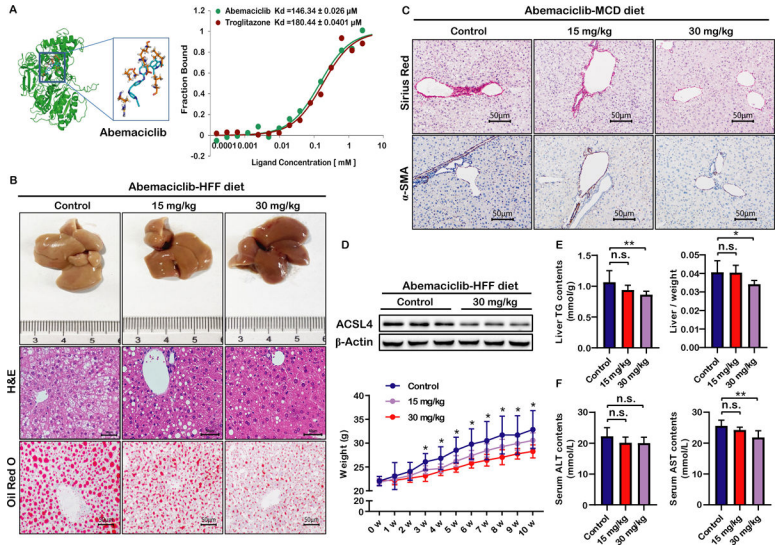

Fig. 4. Abemaciclib treatment inhibited liver steatosis and fibrosis development in HFF and MCD diet mice models.

For the HFF diet, male 9-week-old C57BL/6 mice (n≧10 mice per group) were orally administered with the vehicle or abemaciclib (15 mg/kg and 30 mg/kg) per day. Mice were placed on a HFF diet for the duration of the study, weekly starting at the initiation of the diet. (A) Overall docking views of abemaciclib in the binding pocket of ACSL4, and binding affinity of abemaciclib to ACSL4. (B) Representative macroscopic images, liver H&E images and liver lipid contents as determined by Oil red O staining. n=6 per group. (C) Representative liver fibrosis as determined by Sirius red staining and α-SMA immunohistochemistry. Male 9-week-old C57BL/6 mice were administered with either the vehicle or abemaciclib (15 mg/kg and 30 mg/kg) per day by gavage for 4 weeks. Mice were placed on an MCD diet for the duration of the study. n=6 per group. (D) ACSL4 protein levels (n=3 per group) in liver tissues and body weight changes (n=8 per group). (E) Hepatic triglyceride levels (left), liver to body weight ratios (right). n=8 per group. (F) Serum ALT (left) and AST (right) levels. n=8 per group. Scale bars indicate 50 μm. Error bars represent mean±SD. *denotes $p < 0.05$, **denotes $p < 0.01$. n.s. is defined as not significant.

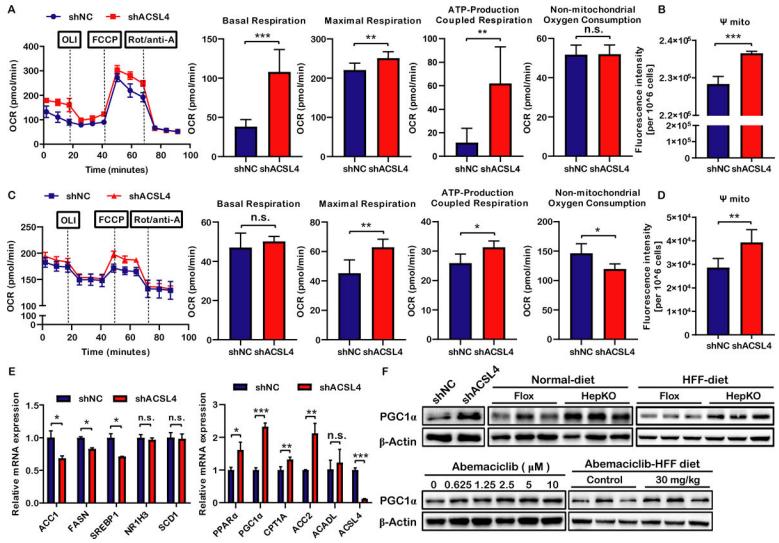

Fig. 5. ACSL4 silencing enhances mitochondrial respiration and promotes β-oxidation *in vitro*.

(A) Oxygen consumption rate (OCR) of HepG2 cells as determined by the Seahorse analyzer. (B) Mitochondrial membrane potential of HepG2 cells as determined by the mitochondrial membrane potential assay kit with JC-1. (C) Oxygen consumption rate (OCR) of human primary hepatocyte-derived liver progenitor-like cells (HepLPCs) as determined by the Seahorse analyzer. (D) Mitochondrial membrane potential of HepLPCs cells as determined by the mitochondrial membrane potential assay kit with JC-1. (E) mRNA expression levels of lipogenesis and fatty acid oxidation associated genes in ACSL4 silenced HepG2 cells, relative to control cells, as determined by qRT-PCR. (F) Protein expression levels of PGC1α in ACSL4 silenced HepG2 cells and in ACSL4 deficient mice liver tissues fed on a normal-diet and HFF diet (up). For HFF diet models, Flox and HepKO mice were fed on a HFF diet for 16 weeks. Protein levels of PGC1α, respond in a dose-dependent manner to abemaciclib *in vitro* and *in vivo* (down). *In vitro*, HepG2 cells were respectively incubated with abemaciclib at 0, 0.625, 1.25, 2.5, 5, 10 μM for 48 h. *In vivo*, C57BL/6 mice administered with the vehicle or abemaciclib (30 mg/kg per day) for ten weeks. Proteins were extracted and subjected to Western blot. Error bars represent mean±SD. *denotes $p < 0.05$, **denotes $p < 0.01$. ***denotes $p < 0.005$. n.s. is defined as not significant.

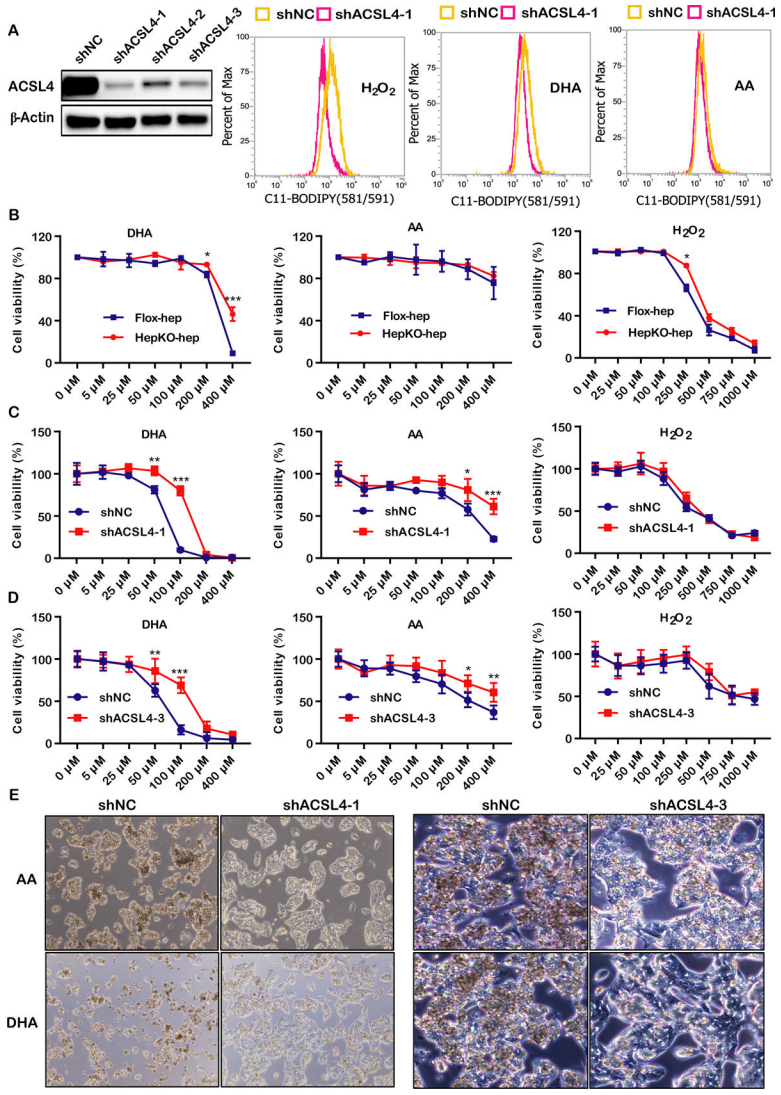

Fig. 6. ACSL4 silencing suppressed lipid peroxidation and the associated cell death.

(A) ACSL4 silencing suppressed lipid ROS production. ACSL4 silenced HepG2 cells were seeded in 12-well plates and cultured overnight. Next day, cells were incubated with C11-BODIPY (581/591) (1 μM) for 30 min at 37 °C in a 5% CO_2 atmosphere. Harvested cells were resuspended in 200 μL fresh PBS, strained through a 40 μM cell strainer and analyzed by flow cytometry. (B-D) Dose dependent effects of ACSL4 on cell viability in mice primary hepatocytes and HepG2 cells. HepG2 cells (C and D) and mice primary hepatocytes (B) obtained from Flox and HepKO mice were treated with AA (0, 5, 25, 50, 100, 200, 400 μM), DHA (0, 5, 25, 50, 100, 200, 400 μM) and H_2O_2 (0, 25, 50, 100, 250, 500, 750, 1000 μM) at indicated concentrations for 48 h and assayed by CCK-8. (E) Macroscopic images of ACSL4 silenced HepG2 cells and its control cells after treatment with AA (400 μM) and DHA (100 μM). Error bars represent mean±SD. *denotes $p < 0.05$, **denotes $p < 0.01$. ***denotes $p < 0.005$.

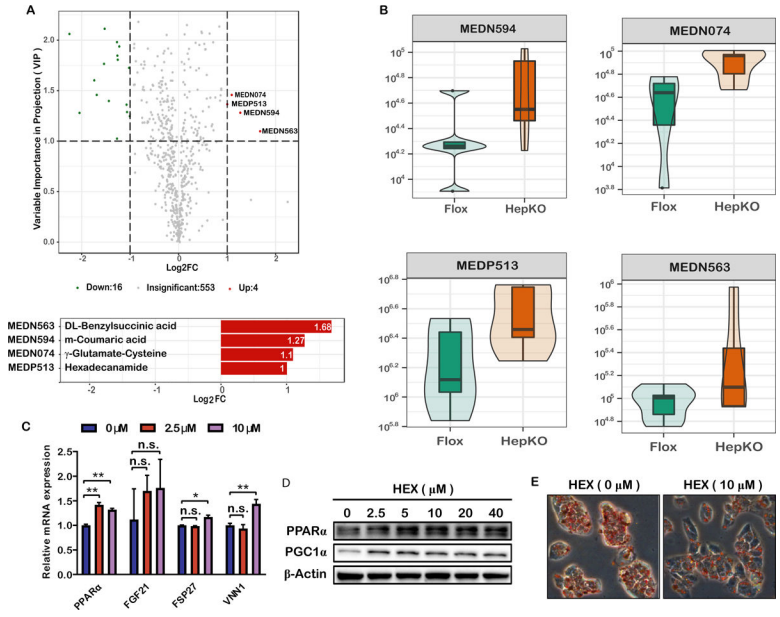

Fig.7. ACSL4 knockdown up-regulated the metabolite hexadecanamide, leading to activation of the PPARα-PGC1α axis.

(A) Bar charts of twenty representative metabolites that were differentially expressed in the livers of Flox and HepKO mice (up). The figure shows the different multiples of each group after log2 transformation (bottom). n=5 per group. (B) Violin plots showing the distribution of values for the significantly up-regulated metabolites of Flox and HepKO mice livers. n=5 per group. (C) PPARα activation by the HEX metabolite. HepG2 cells were treated with HEX (0, 2.5, 10 μM) for 48 h. Total mRNA was extracted and analyzed by qRT-PCR. (D) Dose dependent effects of HEX on the expression levels of PPARα and PGC1α. HepG2 cells were treated with HEX (0, 2.5, 5, 10, 20, 40 μM) for 48 h. Proteins were harvested and assessed by Western blot. (E) Oil red O staining of HepG2 cells treated with HEX and free fatty acids for 24 h. Error bars represent mean±SD. *denotes $p < 0.05$, **denotes $p < 0.01$. n.s. is defined as not significant. HEX, hexadecanamide.

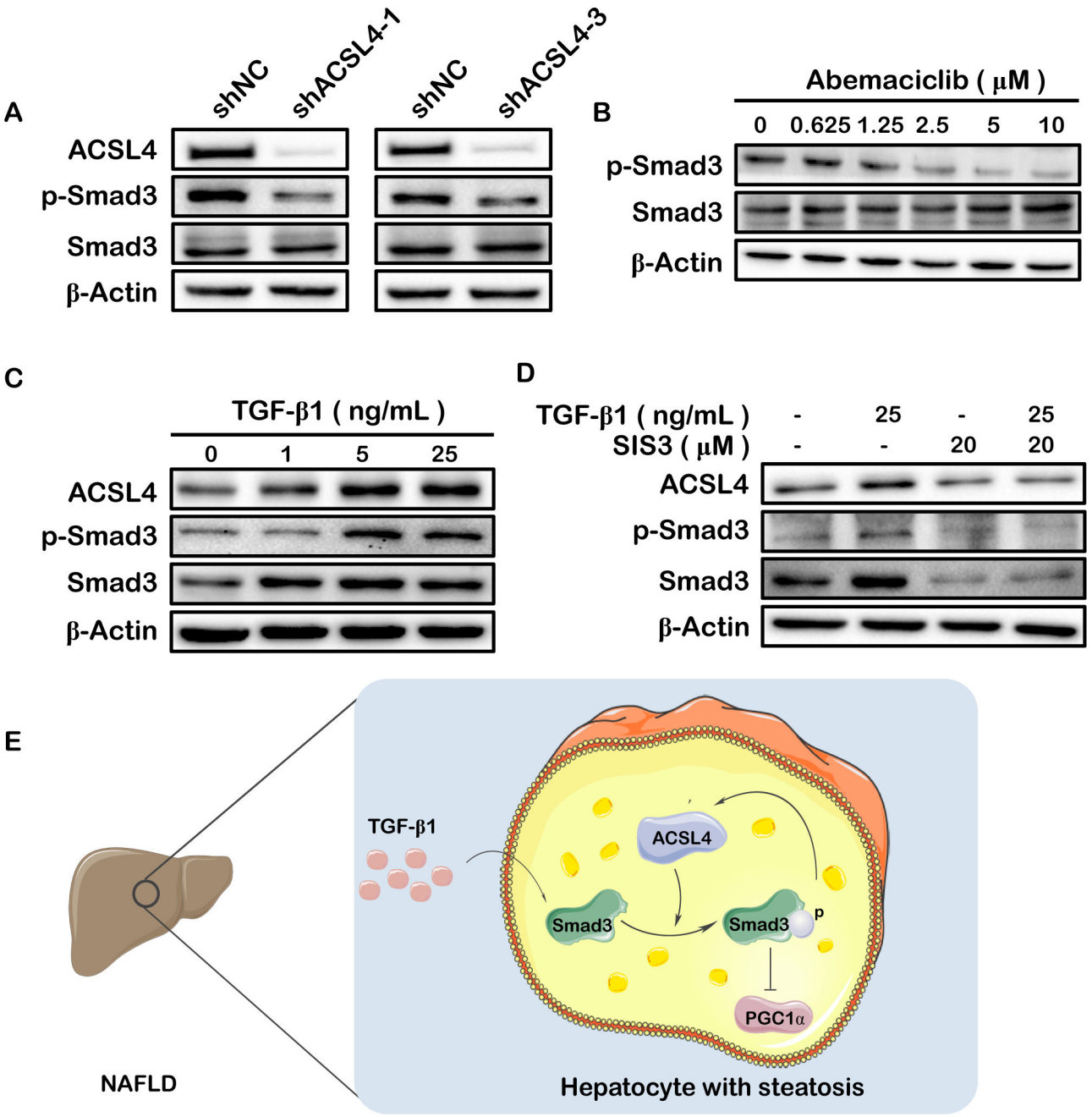

Fig.8. ACSL4 promoted PGC1α expression in a Smad3-dependent manner.

(A-B) Western blot analysis of Smad3, pSmad3 proteins in ACSL4-silenced (A) or abemaciclib- treated (B) HepG2 cells. (C-D) Western blot analysis of ACSL4, Smad3, and pSmad3 proteins in HepG2 cells stimulated by TGF-β1. (E) Summary scheme of the hepatocyte ACSL4/Smad3/PGC1α axis in NAFLD.